



ELSEVIER

Contents lists available at ScienceDirect

Nuclear Instruments and Methods in Physics Research A

journal homepage: www.elsevier.com/locate/nima

The edge transient-current technique (E-TCT) with high energy hadron beam



Andrej Gorišek^{a,*}, Vladimir Cindro^a, Gregor Kramberger^a, Igor Mandić^a, Marko Mikuž^{a,b}, Miha Muškinja^a, Marko Zavrtnik^a

^a J. Stefan Institute, Ljubljana, Slovenia^b University of Ljubljana, Slovenia

ARTICLE INFO

Article history:

Received 26 November 2015

Received in revised form

4 March 2016

Accepted 17 March 2016

Available online 21 March 2016

Keywords:

Solid state detectors

Particle tracking detectors

Silicon

Sensors

CVD diamond sensors

High energy hadron beam

ABSTRACT

We propose a novel way to investigate the properties of silicon and CVD diamond detectors for High Energy Physics experiments complementary to the already well-established E-TCT technique using laser beam. In the proposed setup the beam of high energy hadrons (MIPs) is used instead of laser beam. MIPs incident on the detector in the direction parallel to the readout electrode plane and perpendicular to the edge of the detector. Such experiment could prove very useful to study CVD diamond detectors that are almost inaccessible for the E-TCT measurements with laser due to large band-gap as well as to verify and complement the E-TCT measurements of silicon.

The method proposed is being tested at CERN in a beam of 120 GeV hadrons using a reference telescope with track resolution at the DUT of few μm . The preliminary results of the measurements are presented.

© 2016 Elsevier B.V. All rights reserved.

1. Introduction

Transient current technique is well established method for investigating silicon detectors by studying transient currents induced on electrodes and amplified by a wide range amplifier to deduce the properties of the material (e.g. in [1]). For transient-current technique (TCT) measurement usually either Am alpha source or laser beam incident on electrode are used that deposits charge just under the surface of the electrode which allows one type of carriers to start drifting over the whole volume of the detector.

Recently well-focused laser beams were used to illuminate the edge of the silicon detectors [2]. In this way charge is deposited at a determined depth inside the detector. With a choice of different lasers (red, IR...) different depth of the detector bulk can be accessed. By scanning the laser spot position through the bulk volume, the whole charge drift volume can be studied.

In this paper we propose to use a well collimated high energy hadron beam to study the solid state detectors. Charged hadrons create electron-hole pairs along the path they travel. With the proposed method the drift volume of the electrons and holes can be accessed throughout the volume uniformly along very well defined tracks of charged beam particles that is reconstructed using reference

telescope to accuracy of few microns. Beam particles are usually very parallel with divergences less than a fraction of a mrad.

2. Setup

At CERN SPS H6 beamline in the North Experimental Hall we used the KarTel reference telescope based on 6 Mimosas26 sensor planes of with pixels of size $18\ \mu\text{m}^2$ and area of about $1\ \text{cm} \times 2\ \text{cm}$. Mimosas26 architecture is based on the Mimosas22 (Monolithic Active Pixel Sensor (MAPS) with fast binary readout) and on a prototype circuit named SUZE01 which performs integrated zero suppression. The size of the chip is $13.7\ \text{mm} \times 21.5\ \text{mm}$ and the sensor matrix is composed by 576×1152 pixels of $18.4\ \mu\text{m}$ pitch [6]. Trigger signal is provided by two scintillators placed in front and back of the reference telescope. The size of the scintillators is approximately the size of the Mimosas-26 pixel sensor. An additional silicon pixel detector, attached to a FE-I4 readout chip [7], was installed at the downstream side of the telescope. The FE-I4 chip provides a fast trigger signal when any of the pixels within a settable mask is hit, so called hitbus trigger. This trigger was used to limit the tracks that triggered our system to an area a little bit larger than the detector under test (DUT) studied. This increased significantly the fraction of events with track traversing the DUT.

* Corresponding author.

In current study the DUT was a silicon diode of type W339, produced by STM Microelectronics Catania, of size $5\text{ mm} \times 5\text{ mm}$, $300\text{ }\mu\text{m}$ thickness and oriented along the beam direction. The diode was made of n-type $15\text{ k}\Omega\text{ cm}$ resistivity silicon and had full depletion voltage of $V_{fd}=18\text{ V}$. The diode was operated at 80 V (fully depleted). The cross-section of the DUT hit by the charged particles was $5\text{ mm} \times 300\text{ }\mu\text{m}$. Trigger was implemented with NIM electronic modules (discriminators, logic units, level adapters...) and was effectively a logic AND of both scintillators and hitbus output of FE14. DUT was biased through Bias-T and signal was amplified by wide band amplifier (both by Particulars [3]). Signal was readout by DRS oscilloscope [4] at 1024 samples at 5 GHz.

The Fig. 1 shows schematic view of the CERN SPS beam test setup and in the Fig. 2a photo of this setup can be seen.

3. Analysis and results

Hadrons provided by SPS to H6A beamline had momentum of 120 GeV . The beam had very small divergence of a fraction of a milliradian (see Fig. 3).

The data streams were taken with the telescope and with the DUT independently. Judith software package [5] could not be used in the full extent since the timestamps of the DRS readout board (accurate to 1 ms) were not accurate enough. The delivered beam was divided into spills of few seconds with large gaps without the beam. We identified portions of data in both streams that have

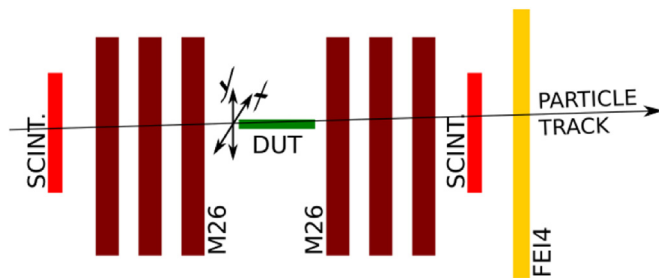


Fig. 1. Schematic view of the test-beam setup comprising of 6 Mimosas-26 planes for tracking, two scintillators for triggering, FE-14 based pixel module for hit-bus region of interest (ROI) selection and DUT on xy translation stages in the middle.

exactly the same number of recorded events within corresponding spills of hadrons delivered to H6A and used only those sections of both streams in further analysis.

Judith software package was also used to align the telescope and to reconstruct clusters in telescope planes and find and fit the charged particle tracks. The only quality criteria applied on events reconstructed was requiring at least 1 track reconstructed in the reference telescope, which further meant that at least 5 clusters reconstructed in Mimosas-26 planes had to fit together into a track [5]. Fig. 4 shows that on average around 10 tracks were reconstructed in frames of reference telescope. For our study lower number would be preferred but this time we were not in control of the H6A beamline. Within one Mimosas26 readout frame we only record the time stamp of the trigger, which corresponds to the first track satisfying the trigger condition only. Two sets of geometric cuts were used to single out events without the signal and events with a large amount of signal in the silicon diode. Narrow virtual

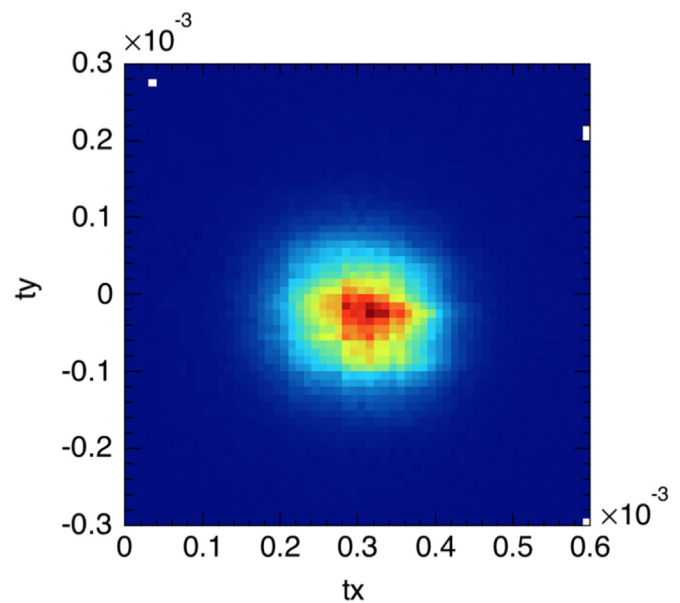


Fig. 3. Dimensionless slope $t_y (=dy/dz)$ vs slope $t_x (=dx/dz)$ of the reconstructed tracks of charged hadrons.

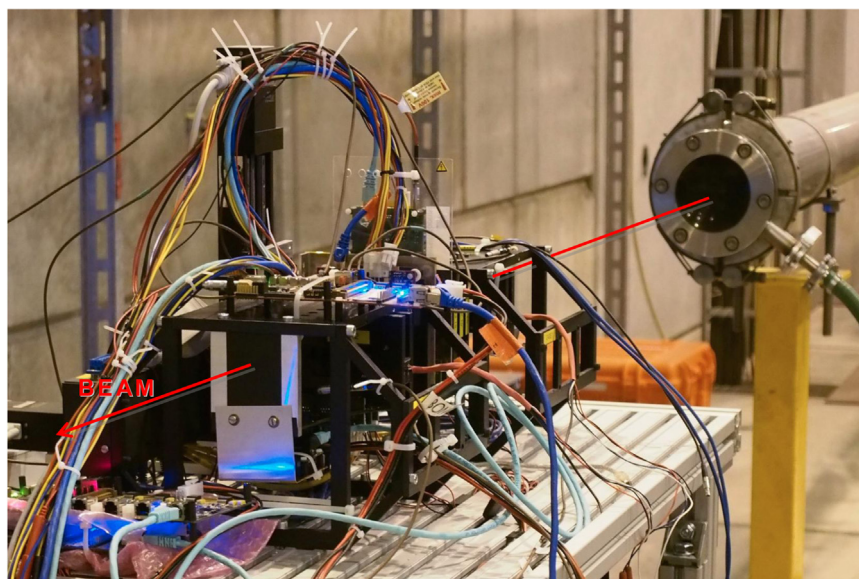


Fig. 2. Photograph of the test-beam setup.

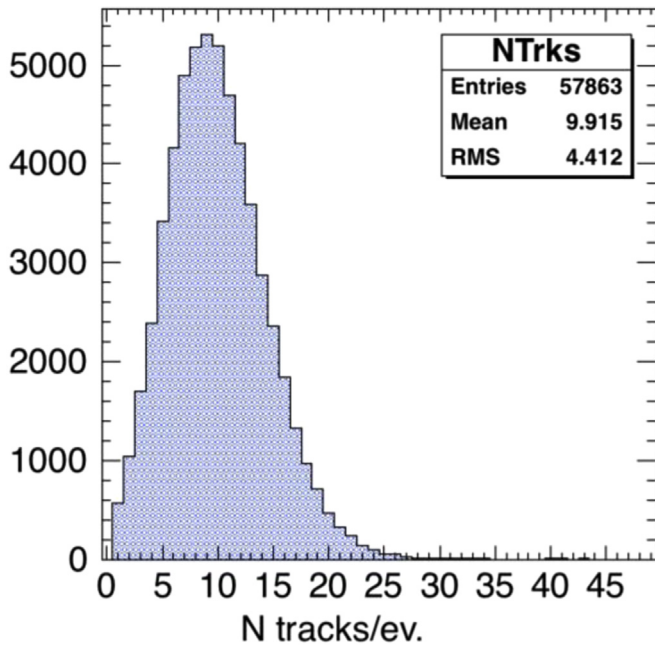


Fig. 4. Distribution of number of tracks reconstructed in a single event. On average around 10 tracks were reconstructed per single event (frame of reference telescope).

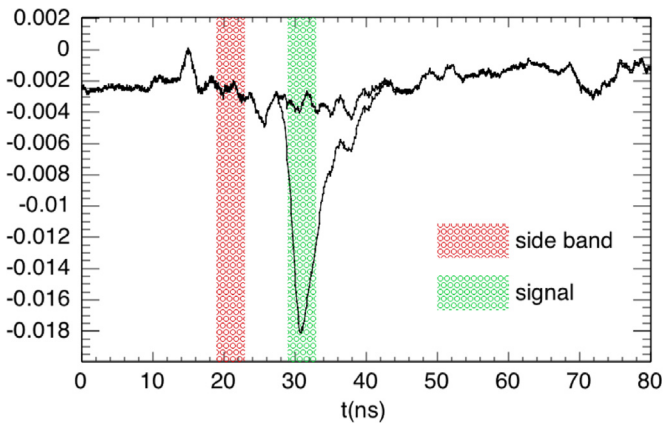


Fig. 5. Average waveform of signals recorded with at least one track traversing geometrical acceptance of the diode forms a clear peak. Waveforms of events with no tracks reconstructed inside the geometric area of the diode and inside a band around it show no peak and they lie on top of each other (obtained with two different set of geometric cuts).

frame of 5 mm width and 300 μm just covered the silicon diode and wide virtual frame of 9 mm width and 800 μm heights covered the diode with a gap around it. The narrow frame was further divided into 7 vertical slices that were named Slice 1 to Slice 7. Fig. 5 shows a set of three average waveforms reconstructed in DRS. The first one which shows a clear peak at ~ 31 ns is obtained by averaging waveforms from events with at least one track inside the narrow frame defined above. The other two averaged waveforms are almost identical and thus hardly separable in Fig. 5. One is obtained by requiring that there are no tracks in selected event inside the narrow frame and the other that there are no tracks in the selected events inside the wide frame. These two waveforms correspond to the baseline recorded by DRS in events where there is no particles traversing the Si diode and were used in the later analysis by subtracting it from the signal waveforms. The area marked in green in the Fig. 5 was used to extract the amplitude of individual waveforms and the area marked in red was used to extract the pedestal in the Fig. 6. The DRS readout recorded only

short fraction of time after the trigger (about 100 ns), on the other hand the telescope frames were 115.2 μs long. The waveforms of the charged particles traversing the Si diode were recorded only in the events when these same particles were the ones that triggered the readout, i.e. only in small fraction of events. This is the reason that the black histogram in the Fig. 6 has a large pedestal

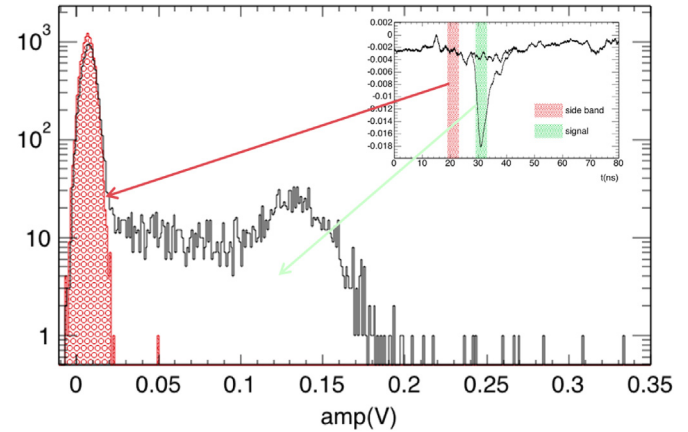


Fig. 6. Histogram of amplitudes of single waveforms inside the green highlighted area and the red highlighted area. The red interval was used for pedestal estimation and the signal distribution was derived from the peak value in the green interval. (For interpretation of the references to color in this figure legend, the reader is referred to the web version of this article.)

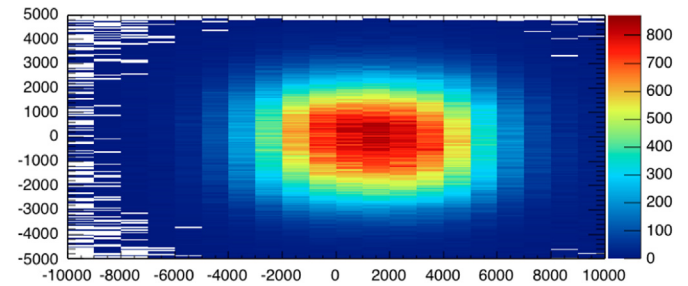


Fig. 7. Distribution of origins of all reconstructed tracks of the charged hadrons.

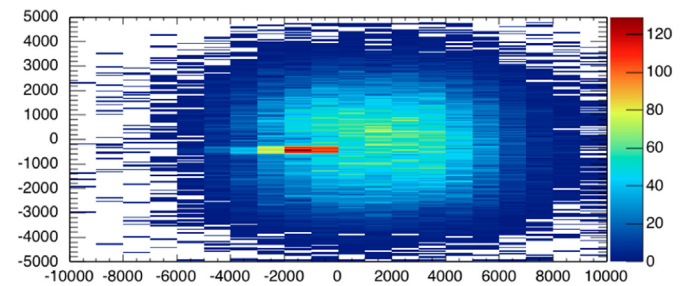


Fig. 8. Distribution of origins of all reconstructed tracks in the events where the amplitude of reconstructed signal in the Si diode was larger than 0.03 V.

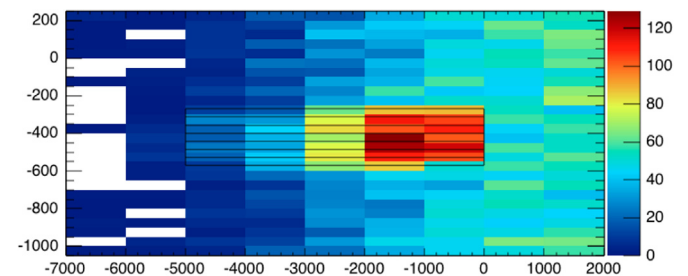


Fig. 9. Side area of the Si diode is divided into 7 slices.

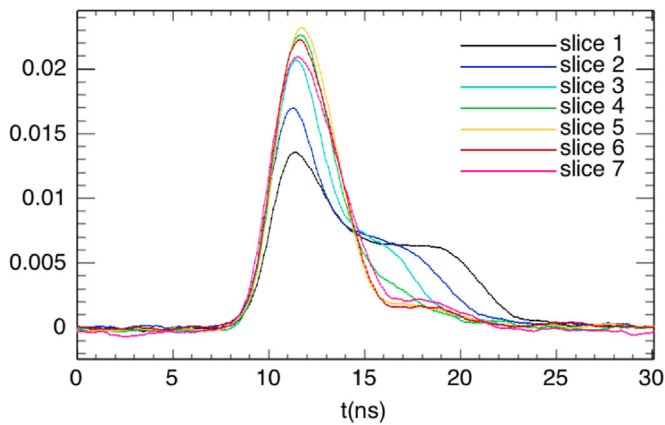


Fig. 10. Average waveform (baseline subtracted) for reconstructed tracks reconstructed in individual slices. Slice 1 has the biggest contribution from slower hole drift which results in a wider plateau while for the Slice 7 the contribution of hole drift is almost gone and most of the signal comes from faster electron drift with a very small remaining contribution from the hole drift.

contribution. The Fig. 7 shows distribution in x and y of all the tracks reconstructed in the reference telescope and the Fig. 8 shows only the tracks reconstructed in the events that had a waveform in DRS reconstructed with larger amplitude than 0.03 V. Fig. 9 shows zoomed area around the narrow frame and partition of it into 7 slices from Slice 1 in the bottom to Slice 7 on top.

Finally the Fig. 10 shows the average waveforms with baseline subtracted for individual slices. Average signal waveform for the Slice 1 has the biggest contribution from slower hole drift while for the Slice 7 the contribution of hole drift is almost gone and most of the signal comes from faster electron drift.

4. Conclusions

It was shown that Edge TCT measurement could be performed in the beam test setup. The proposed method was tested on a

simple silicon diode. This method will be used also on CVD diamond sensors that cannot be easily studied by lasers due to their larger band gap. In case timing precision of signals were improved, this method can also be used for verification/comparison of much simpler laser based Edge TCT for silicon sensors since the amount and distribution of charge created by a minimum ionizing particle (MIP) and very well focused laser beam is somewhat different.

Acknowledgment

This project has received funding from the European Union's Horizon 2020 research and innovation program under grant agreement no. 654168.

References

- [1] I. Mandić, V. Cindro, A. Gorišek, G. Kramberger, M. Mikuž, M. Zavrtanik, V. Fadeyev, H.F.-W. Sadrozinski, M. Christophersen, B. Philips, Nucl. Instrum. Methods Phys. Res. Sect. A Accel. Spectrom. Detect. Assoc. Equip. 751 (2014) 41.
- [2] I. Mandić, V. Cindro, A. Gorišek, G. Kramberger, M. Mikuž, M. Zavrtanik, J. Instrum. 10 (08) (2015), P08004–P08004.
- [3] Particulars, Advanced measurement systems, Ltd. [Online]. Available: (<http://www.particulars.si/index.php>), (accessed: 23.11.15).
- [4] S. Ritt, R. Dinapoli, U. Hartmann, Nucl. Instrum. Methods Phys. Res. Sect. A Accel. Spectrom. Detect. Assoc. Equip. 623 (1) (2010) 486.
- [5] G. McGoldrick, M. Červ, A. Gorišek, Nucl. Instrum. Methods Phys. Res. Sect. A Accel. Spectrom. Detect. Assoc. Equip. 765 (2014) 140.
- [6] J. Baudot, G. Bertolone, A. Brogna, G. Claus, C. Colledani, Y. Degerli, R. De Masi, A. Dorokhov, G. Doziere, W. Dulinski, M. Gelin, M. Goffe, A. Himmi, F. Guilloux, C. Hu-Guo, K. Jaaskelainen, M. Koziel, F. Morel, F. Orsini, M. Specht, I. Valin, G. Voutsinas, M. Winter, First test results Of MIMOSA-26, a fast CMOS sensor with integrated zero suppression and digitized output, in: Proceedings of 2009 IEEE Nuclear Science Symposium Conference Record (NSS/MIC), 2009, pp. 1169–1173.
- [7] M. Garcia-Sciveres, D. Arutinov, M. Barbero, R. Beccherle, S. Dube, D. Elledge, J. Fleury, D. Fougeron, F. Gensolen, D. Gnani, V. Gromov, T. Hemperek, M. Karagounis, R. Kluit, A. Kruth, A. Mekkaoui, M. Menouni, J.-D. Schipper, Nucl. Instrum. Methods Phys. Res. Sect. A Accel. Spectrom. Detect. Assoc. Equip. 636 (1) (2011) S155.